Journal of Visualized Experiments

Expanding the toolkit for in vivo imaging of axonal transport

--Manuscript Draft--

Article Type:	Invited Methods Collection - JoVE Produced Video
Manuscript Number:	JoVE63471R2
Full Title:	Expanding the toolkit for in vivo imaging of axonal transport
Corresponding Author:	Andrew P. Tosolini UNITED KINGDOM
Corresponding Author's Institution:	
Corresponding Author E-Mail:	a.tosolini@ucl.ac.uk
Order of Authors:	Andrew P. Tosolini
	David Villarroel-Campos
	Giampietro Schiavo
	James N. Sleigh
Additional Information:	
Question	**Response**
Please specify the section of the submitted manuscript.	Neuroscience
Please indicate whether this article will be Standard Access or Open Access.	Open Access ($3900)
Please indicate the **city, state/province, and country** where this article will be **filmed**. Please do not use abbreviations.	London, United Kingdom
Please confirm that you have read and agree to the terms and conditions of the author license agreement that applies below:	I agree to the UK Author License Agreement (for UK authors only)
Please confirm that you have read and agree to the terms and conditions of the video release that applies below:	I agree to the Video Release
Please provide any comments to the journal here.	3 of the authors are hosting a methods collection and as per conversations with Ronald Myer this article will be free.

TITLE:

Expanding the Toolkit for *In Vivo* Imaging of Axonal Transport

AUTHORS AND AFFILIATIONS:

Andrew P. Tosolini[1,2], David Villarroel-Campos[1,2,3], Giampietro Schiavo[1,2,3], James N. Sleigh[1,2,3]

[1]Department of Neuromuscular Diseases, UCL Queen Square Institute of Neurology, University College London, UK

[2]UCL Queen Square Motor Neuron Disease Centre, University College London, UK

[3]UK Dementia Research Institute, University College London, UK

Email addresses of co-authors:

David Villarroel-Campos	(david.villarroel.15@ucl.ac.uk)	0000-0003-4250-7216
Giampietro Schiavo	(giampietro.schiavo@ucl.ac.uk)	0000-0002-4319-8745

Corresponding authors:

James N. Sleigh	(j.sleigh@ucl.ac.uk)	0000-0002-3782-9045
Andrew P. Tosolini	(a.tosolini@ucl.ac.uk)	0000-0001-7651-7442

SUMMARY:

Using transgenic fluorescent mice, detailed protocols are described to assess *in vivo* axonal transport of signaling endosomes and mitochondria within motor and sensory axons of the intact sciatic nerve in live animals.

ABSTRACT:

Axonal transport maintains neuronal homeostasis by enabling the bidirectional trafficking of diverse organelles and cargoes. Disruptions in axonal transport have devastating consequences for individual neurons and their networks and contribute to a plethora of neurological disorders. As many of these conditions involve both cell autonomous and non-autonomous mechanisms and often display a spectrum of pathology across neuronal subtypes, methods to accurately identify and analyze neuronal subsets are imperative.

This paper details protocols to assess *in vivo* axonal transport of signaling endosomes and mitochondria in sciatic nerves of anesthetized mice. Stepwise instructions are provided to 1) distinguish motor versus sensory neurons *in vivo, in situ,* and *ex vivo* by using mice that selectively express fluorescent proteins within cholinergic motor neurons; and 2) separately or concurrently assess *in vivo* axonal transport of signaling endosomes and mitochondria. These complementary intravital approaches facilitate the simultaneous imaging of different cargoes in distinct peripheral nerve axons to quantitatively monitor axonal transport in health and disease.

INTRODUCTION:

The peripheral nervous system (PNS) connects the central nervous system (CNS) to its distal targets, permitting the relay of efferent signals to exert motor control and afferent signals to provide sensory feedback. Using the many advances in mouse genetics, scientists have developed different mouse models to investigate many diseases/syndromes afflicting the PNS[1–3]. As most neurodegenerative pathologies are multifactorial with cell autonomous and

non-autonomous pathological contributions[4,5], untangling cell-/neuron-specific pathologies can provide crucial, novel, pathomechanistic clues.

To this end, the development of bacterial artificial chromosome (BAC)-transgenic mice[6] has enabled selective endogenous expression of fluorescent proteins in targeted subsets of neurons. For example, BAC-transgenic mice are available that express green fluorescent protein (GFP) in cholinergic[7] or glycinergic neurons[8] or a variant red fluorescent protein (tdTomato) in parvalbumin-positive neurons[9]. Alternatively, selective neuronal expression of fluorescent proteins can be achieved via Cre-*loxP* technology[10]. For instance, mouse strains expressing Cre-recombinase in subsets of neurons (e.g., choline acetyltransferase (ChAT)-Cre) can be bred with mice that express a fluorescent protein (e.g., tdTomato or GFP) from a constitutive locus (e.g., Gt(ROSA)26Sor) under the control of a transcriptional repressor flanked by loxP sites[11] (e.g., generating mice that express tdTomato only in cholinergic neurons).

Indeed, using Cre-*lox*P recombination, transgenic mice have been generated that express yellow fluorescent protein in axons of the descending corticospinal tract[12]. In addition, recent advances in CRISPR/Cas9 gene editing, such as ORANGE, enable the fluorescent tagging of multiple endogenous neuronal proteins, with expression achievable at nanoscale resolution[13]. Moreover, in combination with Cre-expressing mouse strains, ORANGE-CAKE can be used to tag multiple endogenous proteins in individual neurons[13]. Alternatively, viral-mediated neuronal tracing also allows the labeling of neuronal subsets and can be achieved with targeted combinations of viral serotypes and/or cell-specific promoters[14–17].

In addition to the neuronal labeling methods, mouse lines have also been engineered to express reporter proteins targeting specific organelles, such as mitochondria expressing cyan fluorescent protein (Mito.CFP)[18] or autophagosomes expressing GFP (LC3.GFP)[19]. Moreover, mouse lines have been engineered to assess calcium dynamics specifically in neurons (e.g., Thy1.GCaMP)[20,21]. Altogether, with the advancement of such models, novel experimental applications enable scientists to ask more precise biological and pathological questions about the CNS and PNS.

The main role of peripheral motor nerves is to transmit electrical signals to skeletal muscle to elicit movement. In addition, and occurring over longer time-scales, neurochemical and physiological messages in the form of diverse organelles (e.g., mitochondria, endolysosomes, signaling endosomes) traverse the cytoskeletal network in a uni- or bi-directional manner to help maintain neuronal homeostasis[22–24]. Impairments in axonal transport have disastrous consequences for neuronal health and are linked to many neurodevelopmental and neurodegenerative diseases[25]. At the molecular level, impairments in axonal transport can disrupt physiological events regulating synaptic signaling and plasticity, gene transcription, and local translation throughout the axon[26,27]. While there is a multitude of tools to study these events in cultured cells/neurons[28,29], assessing axonal transport dynamics and axonal-linked biological events *in vivo* are required to confirm key insights into physiological and pathological processes[30].

Over the years, the Schiavo Laboratory has optimized protocols to ask diverse questions about axonal transport[31–36]. These experiments have expanded from the discovery that a

fluorescently labeled atoxic fragment of tetanus neurotoxin (H_CT) is internalized into axon terminals in skeletal muscle through interactions with nidogens and polysialogangliosides[37]. Once internalized, H_CT is retrogradely transported in Rab7-positive, neurotrophin-containing signaling endosomes that are destined for the cell bodies of motor and sensory neurons[38,39,40,41]. In parallel, advances in imaging technology have enabled the real-time imaging of peripheral nerve bundles and individual axons in live, anesthetized mice[30]. The first foray into assessing *in vivo* axonal transport dynamics in pathology revealed presymptomatic impairments in the transport of signaling endosomes and mitochondria in the $SOD1^{G93A}$ mouse model of amyotrophic lateral sclerosis (ALS)[35]. Importantly, these defects are unlikely to simply represent secondary consequences of neurodegeneration, given the finding that motor neuron degeneration can occur in the absence of axonal transport perturbations in a mouse model of Kennedy's disease[42] and a heterozygous mutant FUS model of ALS[43]. Such axonal transport deficits can be remedied in ALS mice using inhibitors of specific kinases[33] or growth factor receptors[34]. Moreover, treating neurons with a specific histone deacetylase blocker alters mitochondrial transport *in vivo*[36].

By using an ever-expanding toolkit for assessing axonal transport dynamics[28,29], this video protocol outlines several applications that will permit further insights into different biological and pathological scenarios. First, transgenic mice that selectively express fluorescent proteins in cholinergic neurons (i.e., motor neurons) are used to discriminate between motor and sensory axons both *in vivo* and *ex vivo*. Fluorescently labeled H_CT is then loaded into signaling endosomes in three transgenic lines to differentiate axonal transport dynamics in distinct peripheral neurons. The next experimental protocol details a multiplex fluorescence approach to assess mitochondrial transport specifically in motor neurons by breeding ChAT.tdTomato mice with Mito-CFP mice. Finally, instructions are provided on how to concurrently image mitochondria and signaling endosomes within the same axon *in vivo*.

PROTOCOL:

All mouse handling and experiments were performed in accordance with the Animals (Scientific Procedures) Act (1986) and were approved by the University College London - Queen Square Institute of Neurology Ethics Committee.

1. Animals

1.1. House all animals in individually ventilated cages in a temperature- and humidity-controlled environment and maintain them on a 12 h light/dark cycle with *ad libitum* access to food and water.

1.2. Use both male and female mice of the following transgenic strains: 1) heterozygous Tg(Chat-EGFP) GH293Gsat/Mmucd mice, referred to as ChAT.eGFP mice; 2) heterozygous B6.Cg-Tg(Hlxb9-GFP)1Tmj/J, referred to as HB9.GFP mice; and 3) heterozygous B6.Cg-Tg(Thy1-CFP/COX8A)S2Lich/J, referred to as Mito.CFP mice.

1.3. Generate ChAT.tdTomato mice by crossing homozygous B6;129S6-*Chat*$^{tm2(cre)Lowl}$/J, referred to as ChAT.Cre mice, with homozygous B6.Cg-*Gt(ROSA)26Sor*$^{tm9(CAG\text{-}tdTomato)Hze}$/J, referred to as Rosa26.tdTomato mice.

1.4. Generate ChAT.tdTomato::Mito.CFP mice by crossing heterozygous ChAT.tdTomato mice with heterozygous Mito.CFP mice.

2. Intramuscular injections of fluorescent H_CT

2.1. Presurgery preparation

2.1.1. Express H_CT (H_CT^{441}, residues 875-1315) fused to an improved cysteine-rich tag in bacteria as a glutathione-S-transferase fusion protein as per [44]. Label H_CT with AlexaFlour555 C_2 maleimide [31], dialyze it in ice-cold dialysis buffer (10 mM HEPES-NaOH, 100 mM NaCl, pH 7.4), freeze it in liquid nitrogen, and store it at -80 °C. Before performing *in vivo* experiments, first test H_CT *in vitro* for successful uptake and transport in primary neurons.

2.1.2. Dilute fluorescent H_CT (e.g., H_CT -555) to a final and experimentally consistent concentration ranging from 2.5 to 10 µg/µL in sterile phosphate-buffered saline (PBS) in a 0.2 mL tube. At this step, add more compounds/factors to the H_CT solution if required (e.g., brain-derived neurotrophic factor).

NOTE: The final volume must be appropriate for the size of the muscle(s) of interest. For example, prepare an injection volume of 3–4 µL for the tibialis anterior (TA) muscle and ~1 µL for the smaller soleus muscle. Keep the working concentration of H_CT between 2.5 and 10 µg/µL regardless of the final volume.

2.1.3. Mix the H_CT solution using a pipette or vortex, and briefly spin down at low speed using a desktop centrifuge to collect the liquid and remove large bubbles. Protect the H_CT from light and transport on ice.

2.1.4. Use a pulled glass micropipette for optimal intramuscular injections into smaller muscles (e.g., soleus) or for intrasciatic nerve injections. Pull graded glass micropipettes (as per [45]) before surgery.

NOTE: To enable pipetting and restrict flow up and out the back of the micropipette, carefully break off a small piece from the sharp tip using fine forceps under a dissecting microscope. Take care to dispose of the broken end in the appropriate bin.

2.1.5. Sterilize and clean all surgical tools prior to use.

2.2. Surgery—intramuscular injections

2.2.1. Prepare for surgery by securing a sterile surgical drape on a heat mat set to 37 °C. Position and focus the operating microscope. For surgery to commence, unpack onto the surgical drape the presterilized surgical tools along with surgical tape, sterile cotton swabs, 70% (v/v) ethanol in water, sterile saline, sutures, and a Hamilton needle or pulled glass micropipettes.

2.2.2. Ensure the anesthetic machine has sufficient oxygen and isoflurane for the duration of the surgical procedure. Direct the flow of anesthesia to the induction chamber and switch on the anesthetic machine.

2.2.2.1. To begin, use an oxygen flow rate of 1–2 L/min and 5% isoflurane. Place the mouse in the induction chamber to initiate anesthesia. When the righting reflex is absent, reduce anesthesia to 2–3% isoflurane, direct the flow of anesthesia to the mouthpiece, and transfer the mouse to the mouthpiece located in a separate area of the surgical space.

2.2.3. Ensure both the corneal and pedal withdrawal reflexes are absent before shaving the area of fur covering the muscle(s) to be injected. When complete, remove as much shaved fur from the mouse as possible using the sticky side of surgical tape, and place the mouse on weighing scales to record its presurgical weight.

2.2.4. Carefully apply eye lubricant using a cotton swab and transfer the mouse and mouthpiece to the surgical area.

NOTE: Try to limit the amount of shaved fur that is also transferred to the surgical area. Use surgical tape to secure the head to the mouthpiece to prevent the mouse from slipping out. Using a separate cotton swab, apply ethanol to the shaved region to sterilize and reduce fur contamination.

2.2.5. Position the body according to the muscle to be injected. For example, for the TA, place the mouse on its back and stretch out the hindlimb at ~10° from the midline. Alternatively, for soleus injections, place the animal on its side and extend the hindlimb at ~45° from the midline. When the hindlimb is in the correct position, use surgical tape across the foot to prevent unwanted movement during surgery.

NOTE: The injection procedures for TA, gastrocnemius, and soleus muscles have been previously detailed[32].

2.2.6. Before making an incision, confirm that the anesthesia is sufficient by testing the pedal withdrawal reflex. Monitor the anesthesia continually and maintain it throughout the surgical procedure with regular assessment of breathing and the withdrawal reflex.

2.2.7. At this point, draw the working H_CT solution into the Hamilton syringe or pulled glass micropipette.

2.2.8. Make a small incision over the muscle(s) of interest in the area(s) that correspond(s) with the motor end plate regions[45–47]. Pierce the external fascia on the muscle and slowly inject the H_CT as per [32]. Leave the syringe/micropipette in position for 5–10 s before slowly withdrawing.

2.2.9. Close the incisions with 1–2 sutures and transfer the mouse to an isolated recovery cage. Monitor the mouse post surgery for a minimum of 30 min, before returning it to the home cage. When the mouse has successfully recovered and postsurgical monitoring is complete, return the cage to normal housing conditions.

3. In vivo axonal transport

3.1. Exposing the sciatic nerve

3.1.1. Set the microscope environmental chamber to 37 °C at least 1 h prior to imaging.

3.1.2. Prepare to expose the sciatic nerve by arranging the surgical drape, tools, tape, sterile cotton swabs, 70% ethanol, and sterile saline around the surgical area. Ensure the anesthetic machine has sufficient stores of oxygen and isoflurane for up to 2 h per mouse. Create a wedge out of parafilm or invisible tape by cutting it into a narrow rectangle (e.g., ~1 cm width) with an angled tip and place it underneath the exposed sciatic nerve to aid the imaging process. Place the induction chamber on top of a heat mat and set it to body temperature.

NOTE: Four hours is ample time for H_CT to have been taken up and retrogradely transported from the site of injection to the sciatic nerve; hence, a single mouse can be readied for re-anesthesia after this time.

3.1.3. Direct the flow of anesthesia into the induction chamber, switch on the anesthetic machine with an oxygen flow rate of 1–2 L/min and 3–4% isoflurane, and place the mouse in the induction chamber to initiate anesthesia.

NOTE: As the *in vivo* axonal transport experiment is a terminal procedure, there is no need to lubricate the eyes.

3.1.4. When the righting reflex is absent, reduce anesthesia to 2–3% isoflurane, direct the flow of anesthesia to the mouthpiece, and transfer the mouse to the mouthpiece. Use surgical tape to secure the head to the mouthpiece, extend the targeted hindlimb at ~45° from the midline, and use surgical tape over the foot to maintain this position.

NOTE: Reduced anesthesia is advantageous at this point as it can limit the impact of breathing artifacts during the imaging process.

3.1.5. Ensure corneal and pedal withdrawal reflexes are absent, and then use scissors to cut away the skin overlying the sciatic nerve[32] (i.e., a large area extending from the central spinal cord to mid-lower hindlimb). Remove the overlying biceps femoris muscle, as well as any other musculature/connective tissue that is near the sciatic nerve. Avoid damaging the sciatic nerve and any blood vessels, especially those located near the lateral aspect of the patella/proximal aspect of the lateral gastrocnemius head.

3.1.6. When the intact sciatic nerve is sufficiently exposed, apply prewarmed sterile saline to the area around the sciatic nerve to prevent desiccation. Use curved forceps to disrupt the deep-lying connective tissue and place the pre-prepared parafilm 'wedge' underneath the nerve. When complete, place saline-soaked cotton wool on the exposed area and move the mouse into the induction chamber positioned on top of the heat mat (set to 37 °C), which should still be filled with isoflurane in O_2.

3.2. *In vivo* axonal imaging

3.2.1. Place a 22 x 64 mm coverglass on the customized microscope stage and secure its position with tape. Select and apply immersion oil to the objective, and then connect the microscope stage to the inverted microscope. Slowly raise the oil-immersed objective until contact is made between the oil and coverglass.

NOTE: Either the 40x, 1.3 numerical aperture (NA) DIC Plan-Apochromat or 63x, 1.4 NA DIC Plan-Apochromat oil-immersion objectives can be used to image *in vivo* transport in the sciatic nerve.

3.2.2. Move the anesthetic mouthpiece onto the microscope stage and secure the anesthesia hoses with tape to prevent disturbance to the anesthesia. Remove the cotton wool from the sciatic nerve and transfer the mouse from the induction chamber to the mouthpiece, with the exposed nerve facing the coverglass. Use surgical tape to ensure the mouse's head is fixed to the mouthpiece and maintain the lowest, effective level of anesthesia. Gently lift the mouse by its tail and add sterile saline to the coverslip near the exposed sciatic nerve to restrict desiccation and aid imaging.

NOTE: Close all doors of the environmental chamber to ensure the area remains at body temperature.

3.2.3. Using the oculars, locate the sciatic nerve, determine the optimal focal point, and select an area of interest containing motile axonal organelles.

3.2.4. Switch to the computer software by clicking the **Acquisition** button (or equivalent), and select an area of interest. Use a digital zoom to obtain a total of >80x magnification and rotate the selected area to horizontally visualize the axons (e.g., right-to-left moving retrograde cargo and left-to-right moving anterograde cargo).

NOTE: The directionality parameters are user-dependent but must remain consistent throughout experiments.

3.2.5. Optimize the signal intensity by adjusting parameters such as **laser intensity (0.2–1%)**, **pinhole aperture (1 AU–max)**, **gain (Master) (700–1000)**, **digital offset (0– 50)**, and **digital gain (1.0–4.0)**. To reduce the potential influence of phototoxicity, maintain **laser intensity** at **≤1%** where possible, with a **maximum laser intensity** of **2%**. Change all other parameters before adjusting the laser intensity for optimal signal detection.

3.2.6. Click the **Regions** box (or equivalent), select a rectangular region of interest, then in the **Acquisition Mode** (or equivalent), set the **frame size** to a minimum **1024 x 1024 pixels**, and commence time-lapse acquisition of 100–1,000 frames.

NOTE: The desired frame acquisition rate is user-dependent (e.g., transport has been successfully assessed with frame rates between 0.1 and 3 s) and can be adjusted with software parameters, such as **region of interest**, **scan speed time**, **acquisition averaging**, and **laser directionality**. For example, to obtain a slower frame rate, increase the height/width of

the region of interest, acquire slower scan speeds, increase the acquisition averaging, and use single laser directionality, and *vice versa* for a faster frame rate. The **frame acquisition rate** must remain consistent across comparable datasets because imaging at different frequencies may cause inconsistencies.

3.2.7. Aim to capture a minimum of 10 motile cargoes from a minimum of three axons per mouse.

NOTE: Based on two-sample, two-sided power calculations (with standard power of 0.8 (1−β) and type I error rate of 5% (α)), sample sizes of 6–8 are sufficient to identify axonal transport differences between wild-type and disease models[35,43].

3.2.8. Once imaging is complete, cull the mouse immediately while under anesthesia (e.g., cervical dislocation). Postmortem tissue, such as muscles and sciatic nerves, can also be harvested for further analysis.

REPRESENTATIVE RESULTS:

This paper details a versatile protocol that expands the *in vivo* axonal transport toolkit. **Figure 1** demonstrates that motor neuron axons can be differentiated from both sensory neuron axons and Schwann cells by using transgenic mice. **Figure 1A** depicts eGFP expression in cholinergic motor axons from a live, anesthetized ChAT.eGFP mouse. **Figure 1B** uses an alternative method to attain tdTomato expression in a freshly excised nerve (i.e., no additional tissue processing) from a ChAT.tdTomato mouse. Hence, using transgenic strains such as ChAT.eGFP, ChAT.tdTomato or Hb9.GFP enables motor axon-specific labeling *in vivo*.

Alternatively, axons can also be identified by injecting tracers/markers (e.g., H_CT[31,32] or adenoviruses encoding eGFP[15]) into skeletal muscles. **Figure 2** highlights such an application, depicting eight robustly expressing ChAT.eGFP-positive axons that contain H_CT-555-positive signaling endosomes (white arrows), ~4 h post probe injection into the TA muscle. Using this experimental design, we could identify TA-innervating α-motor neurons, which are predominantly fast-fatigable[48]. A further five ChAT.eGFP axons with less robust eGFP expression (orange asterisks) were partially out of focus and likely to be located deeper within the sciatic nerve.

Moreover, we identified H_CT-555-positive signaling endosomes in eGFP-negative sensory axons (yellow arrows). As such, using this experimental paradigm, one can specifically assess and compare the axonal transport of signaling endosomes in motor versus sensory neurons *in vivo.* Indeed*,* using this transgenic reporter strain, we discovered that transport of signaling endosomes in ChAT.eGFP-positive motor axons is faster than in ChAT.eGFP-negative sensory axons, which can be reliably differentiated using axon widths[43].

We have previously identified motor neuron axons using the ChAT.eGFP mouse *in vivo*[43]. We now report that HB9.GFP mice can also be used to achieve motor neuron axon identification *in vivo*. Indeed, **Figure 3** presents a series of time-lapse images of HB9.GFP axons containing retrogradely moving H_CT-555-positive signaling endosomes. Note that, unlike ChAT-driven expression, GFP has a more punctate/granular pattern in HB9.GFP axons—the reason for this is unclear.

We have previously described how to monitor *in vivo* mitochondrial dynamics in sciatic nerves via intrasciatic nerve injections of the mitochondrial-targeting dye, tetramethylrhodamine, ethyl ester, perchlorate (TMRE)[32,36]. To reliably differentiate motor versus sensory mitochondria, the Mito.CFP Mouse, which expresses CFP under the *Thy1* promoter[18], can be crossed with transgenic mice that express a fluorescent reporter gene in specific neuronal types. Indeed, by breeding Mito.CFP mice with ChAT.tdTomato mice (referred to as ChAT.tdTomato::Mito.CFP), we could visualize mitochondria specifically in motor axons, as shown in **Figure 4**. In this live multiplex example, five ChAT.tdTomato axons could be visualized, four of which contain CFP-positive mitochondria. Moreover, the node of Ranvier (white arrow in panel iii) could also be identified. Furthermore, the nodes of Ranvier are clearly detectable in ChAT.eGFP, HB9.GFP and Mito.CFP mice (not shown). These double-transgenic strains enable time-lapse intravital imaging of live, anesthetized mice to monitor motor neuron-specific mitochondrial content and axonal transport dynamics.

Finally, signaling endosomes and mitochondria can be concurrently visualized within the same axons *in vivo* by injecting H_CT into the muscles of Mito.CFP mice (**Figure 5**)**.** Intramuscular injections of H_CT-555 were performed in TA muscle in a Mito.CFP mouse ~4 h prior to imaging. Both mitochondria (i panels) and signaling endosomes (ii panels) were simultaneously visualized in muscle-specific axons (i.e., axons innervating the TA). Indeed, anterogradely (yellow triangles) and retrogradely (green triangles and circles) moving organelles as well as stalled organelles (orange triangles and circles) can be observed. Using this experimental paradigm, one can assess the complex functional interactions between axonal mitochondria and signaling endosomes *in vivo*. Overall, we demonstrate several different experimental approaches to assess axonal transport of signaling endosomes and/or mitochondria, specifically in cholinergic motor neurons *in vivo*.

FIGURE AND TABLE LEGENDS:

Figure 1: **Sciatic nerve motor axons**. (**A**) Representative single-plane image of eGFP-positive motor axons obtained *in vivo* from a ChAT.eGFP mouse. (**B**) Representative single-plane image of tdTomato-positive motor axons in an excised sciatic nerve from a ChAT.tdTomato mouse. Distinctions in axon caliber result from differences in mouse age and size. Scale bars = 50 µm. Abbreviations: eGFP = enhanced green fluorescent protein; ChAT = choline O-acetyltransferase.

Figure 2: ***In vivo* axonal transport of signaling endosomes in live sciatic nerve motor and sensory neurons of a ChAT.eGFP mouse**. (**A–C**) Representative images of cholinergic axons expressing eGFP (**A**) and containing H_CT-555-positive signaling endosomes (**B**), and the merge (**C**). The white arrows highlight eGFP-positive motor axons containing H_CT-555-positive signaling endosomes, the blue arrows identify motor axons lacking H_CT-555-positive signaling endosomes, and the yellow arrows highlight eGFP-negative sensory axons transporting H_CT-555-positive signaling endosomes. Orange asterisks identify motor axons with weaker eGFP expression. Scale bar = 25 µm. Abbreviations: eGFP = enhanced green fluorescent protein; ChAT = choline O-acetyltransferase; HcT 555 = tetanus toxin-binding domain.

Figure 3: **Time-lapse image series representing *in vivo* axonal transport of signaling**

endosomes in live motor neurons of an HB9.GFP mouse. (**A–D**) Time-lapse images taken every 3 s depicting motor neuron axons expressing green fluorescent protein (i) and containing H_CT-555-positive signaling endosomes (ii), and the merge (iii). Retrograde movement is from right to left. Scale bar = 10 µm. Abbreviations: GFP = green fluorescent protein; HcT 555 = tetanus toxin-binding domain.

Figure 4: *In vivo* axonal transport of mitochondria in live sciatic nerve motor neurons of a ChAT.tdTomato:: Mito.CFP: mouse. (**A–C**) Representative images of tdTomato-positive motor axons (**A**), containing CFP-positive mitochondria (**B**), and the merge (**C**). The inset images i–iii contain a higher magnification from each panel. The white arrow represents a suspected node of Ranvier. Scale bars = 25 (**A–C**) and 10 µm (i–iii). Abbreviations: ChAT = choline O-acetyltransferase; CFP = cyan fluorescent protein.

Figure 5: Time-lapse image series representing concurrent *in vivo* axonal transport of mitochondria and signaling endosomes in live sciatic nerve motor neurons of a Mito.CFP mouse. (**A–C**) Time-lapse images taken every 3 s depicting axonal transport of both mitochondria (i) and signaling endosomes (ii) within the same sciatic nerve axon (iii). The yellow triangles identify anterogradely moving cargoes, the green circles/triangles identify retrogradely moving cargoes, and the orange circles/triangles identify stationary cargoes. Anterograde movement is from left to right, whereas retrograde movement is in the opposite direction. Scale bar = 10 µm. Abbreviations: HcT 555 = tetanus toxin-binding domain; CFP = cyan fluorescent protein.

DISCUSSION:

This protocol details steps to assess *in vivo* axonal transport of signaling endosomes and mitochondria. Indeed, an experimental setup is provided that enables users to 1) distinguish motor from sensory neurons *in vivo, in situ*, and *ex vivo* by using mice expressing fluorescent reporter proteins selectively expressed in motor neurons; 2) assess *in vivo* axonal transport of signaling endosomes specifically in motor neuron axons using three different transgenic mice; 3) investigate *in vivo* axonal transport of mitochondria specifically in motor neuron axons; and 4) concurrently assess *in vivo* transport dynamics of signaling endosomes and mitochondria within the same axon. This approach has vast potential for investigating axonal transport in basal conditions and can be used to assess pathological perturbations in different diseases affecting peripheral motor and sensory nerves.

Using previous experimental paradigms as a foundation[31,32], here we have detailed novel, robust ways to differentiate axonal transport occurring in motor versus sensory neurons using transgenic reporter mice. Using the Mito.CFP mouse, this approach has been further developed to assess *in vivo* mitochondrial transport by avoiding intrasciatic nerve injections of TMRE[36]. This circumvents possible neural damage and perturbations in axonal transport caused by the intraneuronal injection of the probe. Furthermore, this protocol allows the visualization of axonal transport of multiple organelles in motor axons innervating muscles with distinct physiological properties (e.g., fast-twitch fatigable muscles vs. slow-twitch fatigue-resistant muscles). As such, signaling endosome and/or mitochondrial axonal transport dynamics can be assessed in different subsets of α-motor neurons[48]. Moreover, the axonal transport of those organelles in pathology can also be assessed through crossbreeding with mouse models of different neurodegenerative diseases[1–3].

The axonal transport toolkit is continuously expanding[28,29], and *ex vivo* protocols have been developed to assess transport dynamics using cultured mouse ventral horn explants[49] or excised mouse nerve-muscle preparations[50]. Furthermore, the development of protocols to assess axonal transport in induced human pluripotent stem cell (hiPSC)-derived cortical[51] neurons or hiPSC-derived spinal motor neurons[52] has enabled investigation of human neurons with disease-causing mutations. Such cutting-edge protocols in mouse tissue and human cells can provide critical insights into neuronal function, facilitate novel pathomechanistic discovery in neurodegenerative disease models, and be used to test therapeutic molecules and strategies.

Several **critical steps** need to be followed for the successful implementation of these techniques, and some important notes have been provided in the protocol section. The major requirement for intravital confocal imaging is the equipment to maintain anesthesia and optimum temperature. Indeed, a specialized mobile anesthetic system is needed for 1) induction of anesthesia, 2) dissection/tissue processing (i.e., exposing the sciatic nerve), and 3) maintaining anesthesia during intravital imaging (as previously detailed in [31,32]). Especially when using higher magnification objectives (e.g., 40x or 63x), the depth of anesthesia can impact the image quality, as deeper anesthesia induces large 'gaspy' breaths that result in frequent shifts in focus. Such large movements will undoubtedly impact post imaging transport analyses (e.g., tracking cargoes using the Fiji plugins TrackMate[53] or KymoAnalyzer[54]) as the breathing movements produce artifacts in time-lapse videos that can render them unsuitable for automated tracking or require more time-consuming assessment. Moreover, we have also observed imaging artifacts caused by pulsating arteries within the sciatic nerve, which can only be resolved by choosing a different imaging region. The microscope must be equipped with an environmental chamber capable of maintaining constant body temperature, as temperature and pH influence axonal transport[55]. Furthermore, the application of analgesics post surgery should be avoided, as they can alter transport dynamics[56]. If the experimental design is longitudinal and requires repeated imaging (e.g., [57]), the dissection protocols need to be appropriately adjusted to be minimally invasive and may require additional ethical/licence approval.

Certain **experimental considerations** need to be kept in mind. First, most of the protocols detailed herein involve the use of transgenic mice that possess fluorescent reporter proteins in mitochondria or motor neuron axons. Each of these mouse lines should be bred and imaged as hemi-/heterozygote. The exceptions, however, are the ChAT.Cre and Rosa26.tdTomato mouse lines that can be separately maintained as homozygotes, with the resulting hemizygote offspring enabling tdTomato expression in cholinergic neurons after Cre-*loxP* recombination. When cross-breeding transgenic hemi-/heterozygote mice (e.g., Mito.CFP) with other transgenic hemi-/heterozygote mice (e.g., ChAT.eGFP), one needs to carefully consider the breeding strategy, as obtaining the desired numbers of double-mutant progeny can be time-consuming. Moreover, when breeding the F1 generation of ChAT.Cre and Rosa26.tdTomato mice (i.e., ChAT.tdTomato) with additional transgenic strains (e.g., Mito.CFP), one should expect even fewer mice carrying the desired triple transgenes. In addition, one must also consider the potential fluorophore overlap when breeding two-reporter mice with nearby wavelength properties (e.g., Mito-CFP—excitation: 435 nm,

emission: 485 nm, bred with ChAT.eGFP—excitation: 488 nm, emission: 510 nm), although it may be possible to overcome this problem with spectral unmixing[58].

This technique has some **limitations** to be considered. In this work and our previous protocols[31,32], we have shown how several genetically encoded markers and different staining methods can be used to label and track distinct organelles *in vivo*. However, not all probes are suitable for this experimental approach. We assessed injections into either TA or soleus muscle of cholera toxin beta subunit (CTB)-488 (0.5–1.5 µg/µL ~4 h before imaging), a probe routinely used to label motor neuron cell bodies in *in vivo* retrograde tracer experiments[59,60]. However, when injected alone or co-injected with H_CT-555, the CTB-488 labeling was poor despite using concentrations similar to those used for successful retrograde motor neuron tracing. Thus, we conclude that, despite CTB being an excellent *in vitro* marker of signaling endosomes in neuronal cultures[61], H_CT remains the gold-standard probe to identify signaling endosomes *in vivo* in sciatic nerve axons.

Using different routes, we also tested probes routinely used for labeling lysosomes, such as LysoTracker green DND-26, and markers of active lysosomal hydrolases, such as BODIPY-FL-pepstatin A for Cathepsin D[62] and Magic Red for Cathepsin B, but with no success. We tried intramuscular delivery of BODIPY-FL-pepstatin A (2.5 µg into the TA ~4 h before imaging), as well as intrasciatic injection of 2 µL of LysoTracker (10 µM), BODIPY-FL-pepstatin A (10 µM) or Magic Red (1/10) 30 min and 1 h before imaging. Despite these probes highlighting the nerve, we were unable to find clearly labeled organelles. The probes accumulated around axons, likely being retained by Schwann cells. Hence, the unsuccessful labeling of lysosomes may be due to deficient probe delivery into neurons, although the existence of more suitable concentrations cannot be ruled out. Given that TMRE labeling works under similar conditions (i.e., intrasciatic injections), the labeling intensity may be dye-dependent and must be tested for each marker independently. However, we conclude that targeting lysosomes *in vivo* with these probes is not feasible at the concentrations stated above.

Methods of anesthesia can alter distinct physiological readouts (e.g., cochlea function[63] and cortical electrophysiology[64]); however, whether anesthesia influences axonal transport in the sciatic nerve is currently unknown. Given the reduced neuromuscular activity under isoflurane-induced anesthesia, it is possible that transport kinetics differ compared to the wakeful state. However, the only *in vivo* study that has directly investigated this revealed that transport of dense core vesicles in thalamocortical projections does not differ between anesthetized and awake mice[65]. Furthermore, because distinctions in transport between wild-type and disease model mice are detectable under anesthesia[35,43], it is clear that isoflurane exposure does not prevent the identification of perturbances in signaling endosome or mitochondrial trafficking.

This protocol has **other potential applications**, which have been described below. Breeding of the transgenic mice described in this protocol (e.g., Mito.CFP, ChAT.eGFP) with neurodegenerative disease mouse models[1–3] will enable neuron subtype- and/or cargo-specific investigations. Moreover, recently developed mouse Cre lines[66] would also permit the visualization of fluorescent reporter proteins in distinct sensory axon populations. For example, Rosa26.tdTomato mice can be crossed with a neuropeptide Y receptor-2-expressing (Npy2r).Cre mouse to enable tdTomato fluorescence in myelinated A-fiber nociceptors[67].

Furthermore, temporal control can also be achieved by using inducible Cre systems (e.g., tamoxifen)[68]. Another potential application relies on the availability of transgenic mice expressing fluorescent reporter proteins in Schwann cells. Indeed, S100-GFP[69] and PLP-GFP[70] mice enable *in vivo* and/or *in situ* imaging of Schwann cells and have been at the forefront of research involved in Schwann cell migration during peripheral nerve regeneration.

In addition to these applications and complementing the Mito.CFP mouse is the availability of several transgenic mouse lines that express fluorescent proteins in distinct organelles, such as mitochondria and autophagosomes. For example, investigating *in vivo* mitochondrial transport might be possible with the mito::mKate2 mouse[71] or the photoconvertible mitoDendra mouse[57]. Moreover, *in vivo* mitophagosome transport may be possible using the pH-sensitive mito-Keima mouse[72] and the mito-QC mouse[73] for mitophagy analyses. Furthermore, the lysosomal labeling difficulties we encountered may be overcome by using mice expressing LAMP1-GFP, with the caveat that LAMP1 is also present in endocytic organelles distinct from lysosomes[74]. In summary, we have provided novel ways to assess axonal transport of multiple organelles in specific peripheral nerve axons and diverse transgenic mice. We believe that these can be extremely useful experimental tools to understand the basal physiology of axons *in vivo* and can untangle important pathomechanisms driving the neurodegeneration of peripheral nerves.

ACKNOWLEDGMENT:

We would like to thank Robert M. Brownstone (Queen Square Institute of Neurology, University College London) for sharing the ChAT-eGFP, ChAT.Cre and Rosa26.tdTomato mice, and Pietro Fratta (Queen Square Institute of Neurology, University College London) for sharing the HB9.GFP mouse. We would like to thank Elena Rhymes, Charlotte Kremers, and Qiuhan Lang (Queen Square Institute of Neurology, University College London) for critical reading of the manuscript. This work was supported by a Junior Non-Clinical Fellowship from the Motor Neuron Disease Association (UK) (Tosolini/Oct20/973-799) (APT), the Wellcome Trust Senior Investigator Awards (107116/Z/15/Z and 223022/Z/21/Z) (GS), a UK Dementia Research Institute Foundation award (GS); and a Medical Research Council Career Development Award (MR/S006990/1) (JNS).

DISCLOSURES:

The authors have no conflicts of interest.

REFERENCES:

1. Webster, R. G. Animal models of the neuromuscular junction, vitally informative for understanding function and the molecular mechanisms of congenital myasthenic syndromes. *International Journal of Molecular Sciences.* **19** (5), 1326 (2018).
2. Sleigh, J. N., Gillingwater, T. H., Talbot, K. The contribution of mouse models to understanding the pathogenesis of spinal muscular atrophy. *Disease Models & Mechanisms.* **4** (4), 457–467 (2011).
3. De Giorgio, F., Maduro, C., Fisher, E. M. C., Acevedo-Arozena, A. Transgenic and physiological mouse models give insights into different aspects of amyotrophic lateral sclerosis. *Disease Models & Mechanisms.* **12** (1), dmm037424 (2019).
4. Ilieva, H., Polymenidou, M., Cleveland, D. W. Non-cell autonomous toxicity in

610 neurodegenerative disorders: ALS and beyond. *The Journal of Cell Biology.* **187** (6), 761–772
611 (2009).
612 5. Brown, R. H., Al-Chalabi, A. Amyotrophic lateral sclerosis. *The New England Journal of*
613 *Medicine.* **377** (2), 162–172 (2017).
614 6. Gong, S. et al. A gene expression atlas of the central nervous system based on bacterial
615 artificial chromosomes. *Nature.* **425** (6961), 917–925 (2003).
616 7. Tallini, Y. N. et al. BAC transgenic mice express enhanced green fluorescent protein in
617 central and peripheral cholinergic neurons. *Physiological Genomics.* **27** (3), 391–397 (2006).
618 8. Zeilhofer, H. U. et al. Glycinergic neurons expressing enhanced green fluorescent
619 protein in bacterial artificial chromosome transgenic mice. *The Journal of Comparative*
620 *Neurology.* **482** (2), 123–141 (2005).
621 9. Kaiser, T., Ting, J. T., Monteiro, P., Feng, G. Transgenic labeling of parvalbumin-
622 expressing neurons with tdTomato. *Neuroscience.* **321**, 236–245 (2016).
623 10. Zheng, B., Sage, M., Sheppeard, E. A., Jurecic, V., Bradley, A. Engineering mouse
624 chromosomes with Cre-loxP: range, efficiency, and somatic applications. *Molecular and*
625 *Cellular Biology.* **20** (2), 648–655 (2000).
626 11. Madisen, L. et al. A robust and high-throughput Cre reporting and characterization
627 system for the whole mouse brain. *Nature Neuroscience.* **13** (1), 133–140 (2010).
628 12. Bareyre, F. M., Kerschensteiner, M., Misgeld, T., Sanes, J. R. Transgenic labeling of the
629 corticospinal tract for monitoring axonal responses to spinal cord injury. *Nature Medicine.* **11**
630 (12), 1355–1360 (2005).
631 13. Willems, J. et al. ORANGE: A CRISPR/Cas9-based genome editing toolbox for epitope
632 tagging of endogenous proteins in neurons. *PLoS Biology.* **18** (4), e3000665 (2020).
633 14. Huh, Y., Oh, M. S., Leblanc, P., Kim, K.-S. Gene transfer in the nervous system and
634 implications for transsynaptic neuronal tracing. *Expert Opinion on Biological Therapy.* **10** (5),
635 763–772 (2010).
636 15. Tosolini, A. P., Morris, R. Targeting motor end plates for delivery of adenoviruses: an
637 approach to maximize uptake and transduction of spinal cord motor neurons. *Scientific*
638 *Reports.* **6**, 33058 (2016).
639 16. Andrews, M. R. Gene therapy in the CNS-one size does not fit all. *Gene Therapy.* **28**
640 (7–8), 393–395 (2021).
641 17. Kügler, S. Tissue-specific promoters in the CNS. *Methods in Molecular Biology.* **1382**,
642 81–91 (2016).
643 18. Misgeld, T., Kerschensteiner, M., Bareyre, F. M., Burgess, R. W., Lichtman, J. W.
644 Imaging axonal transport of mitochondria in vivo. *Nature Methods.* **4** (7), 559–561 (2007).
645 19. Mizushima, N., Yamamoto, A., Matsui, M., Yoshimori, T., Ohsumi, Y. In vivo analysis of
646 autophagy in response to nutrient starvation using transgenic mice expressing a fluorescent
647 autophagosome marker. *Molecular Biology of the Cell.* **15** (3), 1101–1111 (2004).
648 20. Dana, H. et al. Thy1-GCaMP6 transgenic mice for neuronal population imaging in vivo.
649 *PLoS One* **9** (9), e108697 (2014).
650 21. Chen, Q. et al. Imaging neural activity using Thy1-GCaMP transgenic mice. *Neuron.* **76**
651 (2), 297–308 (2012).
652 22. Maday, S., Twelvetrees, A. E., Moughamian, A. J., Holzbaur, E. L. F. Axonal transport:
653 cargo-specific mechanisms of motility and regulation. *Neuron.* **84** (2), 292–309 (2014).
654 23. Terenzio, M., Schiavo, G., Fainzilber, M. Compartmentalized signaling in neurons: from
655 cell biology to neuroscience. *Neuron.* **96** (3), 667–679 (2017).
656 24. Abouward, R., Schiavo, G. Walking the line: mechanisms underlying directional mRNA

transport and localisation in neurons and beyond. *Cellular and Molecular Life Sciences.* **78** (6), 2665–2681 (2021).
25. Sleigh, J. N., Rossor, A. M., Fellows, A. D., Tosolini, A. P., Schiavo, G. Axonal transport and neurological disease. *Nature Reviews. Neurology.* **15** (12), 691–703 (2019).
26. Bronfman, F. C., Moya-Alvarado, G. BDNF/TrkB signaling endosomes mediate long-distance dendritic growth by activating CREB/PI3K-mTOR-dependent translation in neuronal cell bodies. *BioRxiv*. doi:10.1101/2020.08.22.262923 (2020).
27. Nagano, S., Araki, T. Axonal Transport and Local Translation of mRNA in Neurodegenerative Diseases. *Frontiers in Molecular Neuroscience.* **14**, 697973 (2021).
28. Boecker, C. A., Olenick, M. A., Gallagher, E. R., Ward, M. E., Holzbaur, E. L. F. ToolBox: Live Imaging of intracellular organelle transport in induced pluripotent stem cell-derived neurons. *Traffic.* **21** (1), 138–155 (2020).
29. Surana, S. et al. The evolution of the axonal transport toolkit. *Traffic.* **21** (1), 13–33 (2020).
30. Sleigh, J. N., Vagnoni, A., Twelvetrees, A. E., Schiavo, G. Methodological advances in imaging intravital axonal transport. *F1000Research.* **6**, 200, doi:10.12688/f1000research.10433.1 (2017).
31. Gibbs, K. L., Kalmar, B., Sleigh, J. N., Greensmith, L., Schiavo, G. *In vivo* imaging of axonal transport in murine motor and sensory neurons. *Journal of Neuroscience Methods.* **257**, 26–33 (2016).
32. Sleigh, J. N., Tosolini, A. P., Schiavo, G. *In vivo* imaging of anterograde and retrograde axonal transport in rodent peripheral nerves. *Methods in Molecular Biology.* **2143**, 271–292 (2020).
33. Gibbs, K. L. et al. Inhibiting p38 MAPK alpha rescues axonal retrograde transport defects in a mouse model of ALS. *Cell Death & Disease.* **9** (6), 596 (2018).
34. Fellows, A. D., Rhymes, E. R., Gibbs, K. L., Greensmith, L., Schiavo, G. IGF1R regulates retrograde axonal transport of signalling endosomes in motor neurons. *EMBO Reports.* **21** (3), e49129 (2020).
35. Bilsland, L. G., Sahai, E., Kelly, G., Golding, M., Greensmith, L., Schiavo, G. Deficits in axonal transport precede ALS symptoms in vivo. *Proceedings of the National Academy of Sciences of the United States of America.* **107** (47), 20523–20528 (2010).
36. Kalinski, A. L. et al. Deacetylation of Miro1 by HDAC6 blocks mitochondrial transport and mediates axon growth inhibition. *The Journal of Cell Biology.* **218** (6), 1871–1890 (2019).
37. Bercsenyi, K. et al. Tetanus toxin entry. Nidogens are therapeutic targets for the prevention of tetanus. *Science.* **346** (6213), 1118–1123 (2014).
38. Deinhardt, K. et al. Rab5 and Rab7 control endocytic sorting along the axonal retrograde transport pathway. *Neuron.* **52** (2), 293–305 (2006).
39. Debaisieux, S., Encheva, V., Chakravarty, P., Snijders, A. P., Schiavo, G. Analysis of signaling endosome composition and dynamics using SILAC in embryonic stem cell-derived neurons. *Molecular & Cellular Proteomics.* **15** (2), 542–557 (2016).
40. Surana, S. et al. The travel diaries of tetanus and botulinum neurotoxins. *Toxicon.* **147**, 58–67 (2018).
41. Villarroel-Campos, D., Schiavo, G., Lazo, O. M. The many disguises of the signalling endosome. *FEBS Letters.* **592** (21), 3615–3632 (2018).
42. Malik, B. et al. Absence of disturbed axonal transport in spinal and bulbar muscular atrophy. *Human Molecular Genetics.* **20** (9), 1776–1786 (2011).
43. Sleigh, J. N. et al. Mice carrying ALS mutant TDP-43, but not mutant FUS, display in

vivo defects in axonal transport of signaling endosomes. *Cell Reports.* **30** (11), 3655–3662.e2 (2020).
44. Restani, L. et al. Botulinum neurotoxins A and E undergo retrograde axonal transport in primary motor neurons. *PLoS Pathogens.* **8** (12), e1003087 (2012).
45. Mohan, R., Tosolini, A. P., Morris, R. Intramuscular injections along the motor end plates: a minimally invasive approach to shuttle tracers directly into motor neurons. *Journal of Visualized Experiments: JoVE.* (101), e52846 (2015).
46. Tosolini, A. P., Mohan, R., Morris, R. Targeting the full length of the motor end plate regions in the mouse forelimb increases the uptake of fluoro-gold into corresponding spinal cord motor neurons. *Frontiers in Neurology.* **4**, 58, doi:10.3389/fneur.2013.00058 (2013).
47. Mohan, R., Tosolini, A. P., Morris, R. Targeting the motor end plates in the mouse hindlimb gives access to a greater number of spinal cord motor neurons: an approach to maximize retrograde transport. *Neuroscience.* **274**, 318–330 (2014).
48. Stifani, N. Motor neurons and the generation of spinal motor neuron diversity. *Frontiers in Cellular Neuroscience.* **8**, 293 (2014).
49. Altman, T., Maimon, R., Ionescu, A., Pery, T. G., Perlson, E. Axonal transport of organelles in motor neuron cultures using microfluidic chambers system. *Journal of Visualized Experiments: JoVE.* (159), doi:10.3791/60993 (2020).
50. Boyer, N. P., Azcorra, M., Jung, P., Brown, A. Imaging and analysis of neurofilament transport in excised mouse tibial nerve. *Journal of Visualized Experiments: JoVE.* (162), doi:10.3791/61264 (2020).
51. Mou, Y., Mukte, S., Chai, E., Dein, J., Li, X.-J. Analyzing mitochondrial transport and morphology in human induced pluripotent stem cell-derived neurons in hereditary spastic paraplegia. *Journal of Visualized Experiments: JoVE.* (156), doi:10.3791/60548 (2020).
52. Stoklund Dittlau, K. *et al.* Generation of human motor units with functional neuromuscular junctions in microfluidic devices. *Journal of Visualized Experiments: JoVE.* (175), doi:10.3791/62959 (2021).
53. Tinevez, J.-Y. et al. TrackMate: An open and extensible platform for single-particle tracking. *Methods.* **115**, 80–90 (2017).
54. Neumann, S., Chassefeyre, R., Campbell, G. E., Encalada, S. E. KymoAnalyzer: a software tool for the quantitative analysis of intracellular transport in neurons. *Traffic.* **18** (1), 71–88 (2017).
55. Bohnert, S., Schiavo, G. Tetanus toxin is transported in a novel neuronal compartment characterized by a specialized pH regulation. *The Journal of Biological Chemistry.* **280** (51), 42336–42344 (2005).
56. Kanai, A. et al. Low-concentration lidocaine rapidly inhibits axonal transport in cultured mouse dorsal root ganglion neurons. *Anesthesiology.* **95** (3), 675–680 (2001).
57. Bolea, I., Gan, W.-B., Manfedi, G., Magrané, J. Imaging of mitochondrial dynamics in motor and sensory axons of living mice. *Methods in Enzymology.* **547**, 97–110 (2014).
58. Cohen, S., Valm, A. M., Lippincott-Schwartz, J. Multispectral live-cell imaging. *Current Protocols in Cell Biology.* **79** (1), e46 (2018).
59. Blum, J. A. et al. Single-cell transcriptomic analysis of the adult mouse spinal cord reveals molecular diversity of autonomic and skeletal motor neurons. *Nature Neuroscience.* **24** (4), 572–583 (2021).
60. Xu, J. et al. An approach to maximize retrograde transport based on the spatial distribution of motor endplates in mouse hindlimb muscles. *Frontiers in Cellular Neuroscience.* **15**, 707982 (2021).

61. Wang, T. et al. Flux of signalling endosomes undergoing axonal retrograde transport is encoded by presynaptic activity and TrkB. *Nature Communications.* **7**, 12976 (2016).
62. Chen, C. S., Chen, W. N., Zhou, M., Arttamangkul, S., Haugland, R. P. Probing the cathepsin D using a BODIPY FL-pepstatin A: applications in fluorescence polarization and microscopy. *Journal of Biochemical and Biophysical Methods.* **42** (3), 137–151 (2000).
63. Cederholm, J. M. E. et al. Differential actions of isoflurane and ketamine-based anaesthetics on cochlear function in the mouse. *Hearing Research.* **292** (1–2), 71–79 (2012).
64. Michelson, N. J., Kozai, T. D. Y. Isoflurane and ketamine differentially influence spontaneous and evoked laminar electrophysiology in mouse V1. *Journal of Neurophysiology.* **120** (5), 2232–2245 (2018).
65. Knabbe, J., Nassal, J. P., Verhage, M., Kuner, T. Secretory vesicle trafficking in awake and anaesthetized mice: differential speeds in axons versus synapses. *The Journal of Physiology.* **596** (16), 3759–3773 (2018).
66. Gong, S. et al. Targeting Cre recombinase to specific neuron populations with bacterial artificial chromosome constructs. *The Journal of Neuroscience.* **27** (37), 9817–9823 (2007).
67. Arcourt, A. *et al.* Touch receptor-derived sensory information alleviates acute pain signaling and fine-tunes nociceptive reflex coordination. *Neuron.* **93** (1), 179–193 (2017).
68. Valny, M., Honsa, P., Kirdajova, D., Kamenik, Z., Anderova, M. Tamoxifen in the mouse brain: implications for fate-mapping studies using the tamoxifen-inducible Cre-loxP system. *Frontiers in Cellular Neuroscience.* **10**, 243 (2016).
69. Hayashi, A. *et al.* A double-transgenic mouse used to track migrating Schwann cells and regenerating axons following engraftment of injured nerves. *Experimental Neurology.* **207** (1), 128–138 (2007).
70. Chen, B., Chen, Q., Parkinson, D. B., Dun, X.-P. Analysis of schwann cell migration and axon regeneration following nerve injury in the sciatic nerve bridge. *Frontiers in Molecular Neuroscience.* **12**, 308 (2019).
71. Barrasso, A. P., Tong, X., Poché, R. A. The mito::mKate2 mouse: A far-red fluorescent reporter mouse line for tracking mitochondrial dynamics in vivo. *Genesis.* **56** (2), doi:10.1002/dvg.23087 (2018).
72. Sun, N. et al. A fluorescence-based imaging method to measure in vitro and in vivo mitophagy using mt-Keima. *Nature Protocols.* **12** (8), 1576–1587 (2017).
73. McWilliams, T. G. et al. mito-QC illuminates mitophagy and mitochondrial architecture in vivo. *The Journal of Cell Biology.* **214** (3), 333–345 (2016).
74. Cheng, X.-T. et al. Characterization of LAMP1-labeled nondegradative lysosomal and endocytic compartments in neurons. *The Journal of Cell Biology.* **217** (9), 3127–3139 (2018).

Figure 1

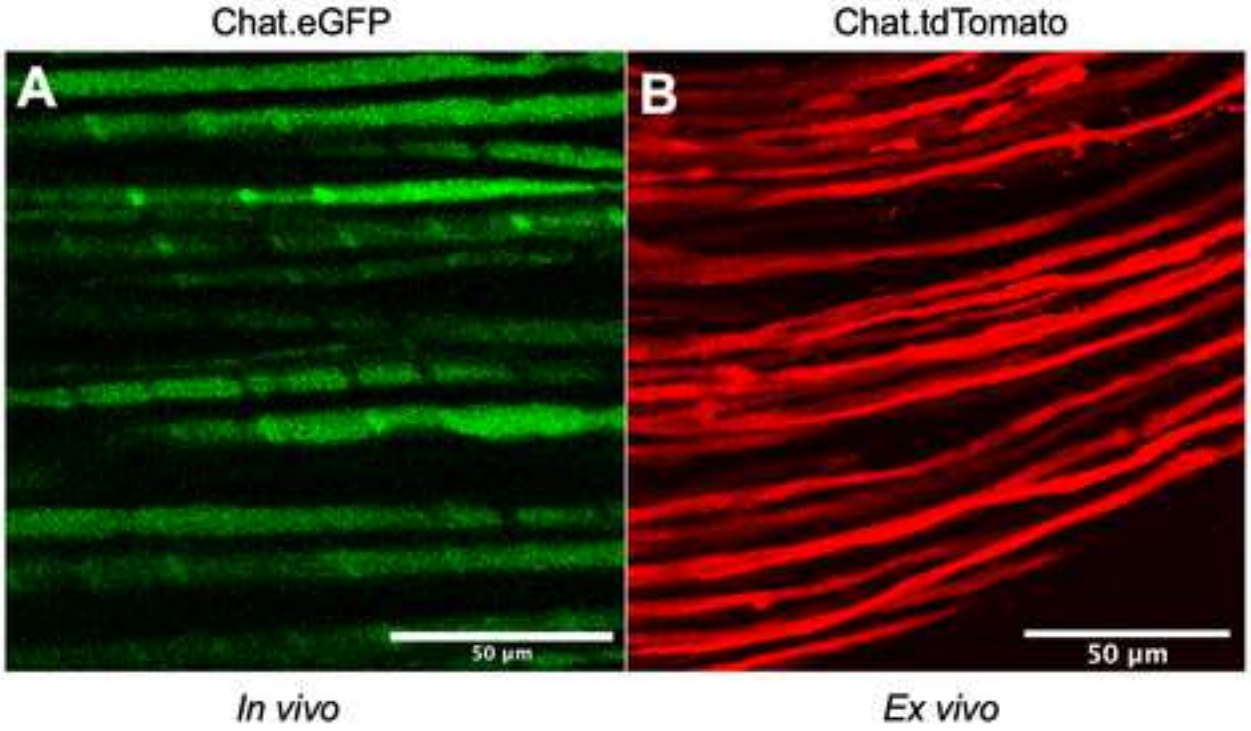

Figure 2

Click here to access/download;Figure;Figure 2.tiff

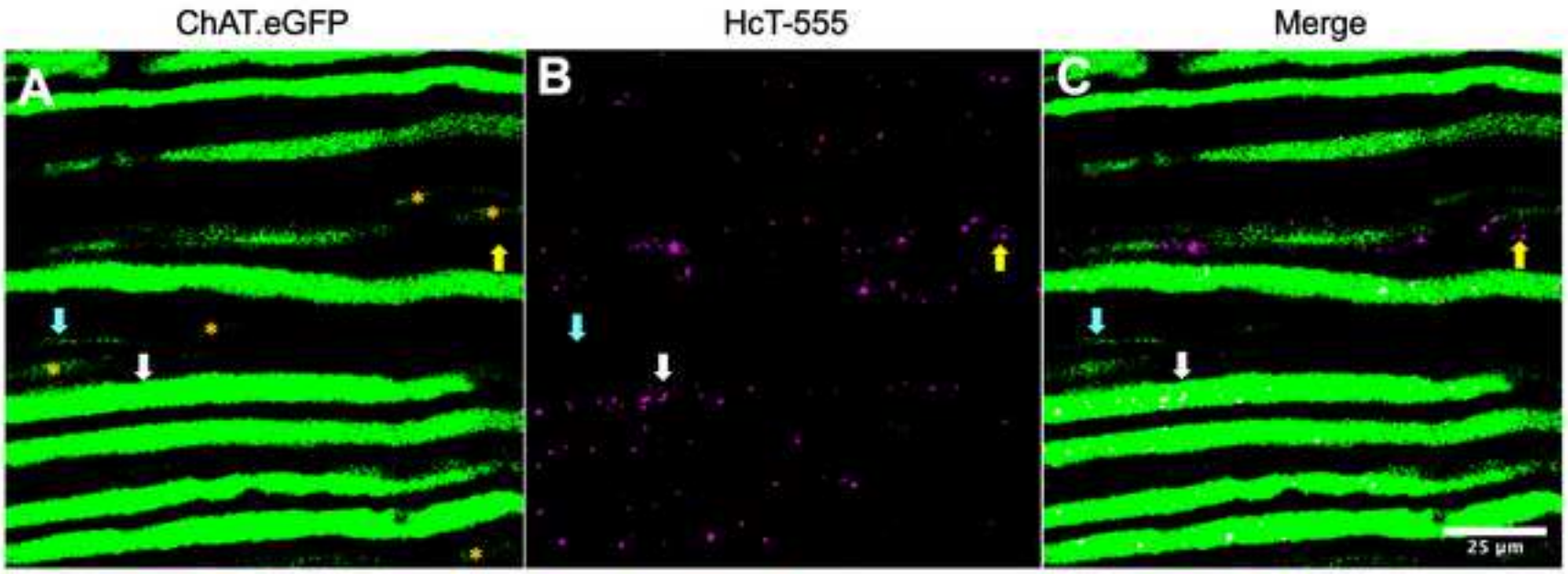

Figure 3

Click here to access/download;Figure;Figure 3.tiff

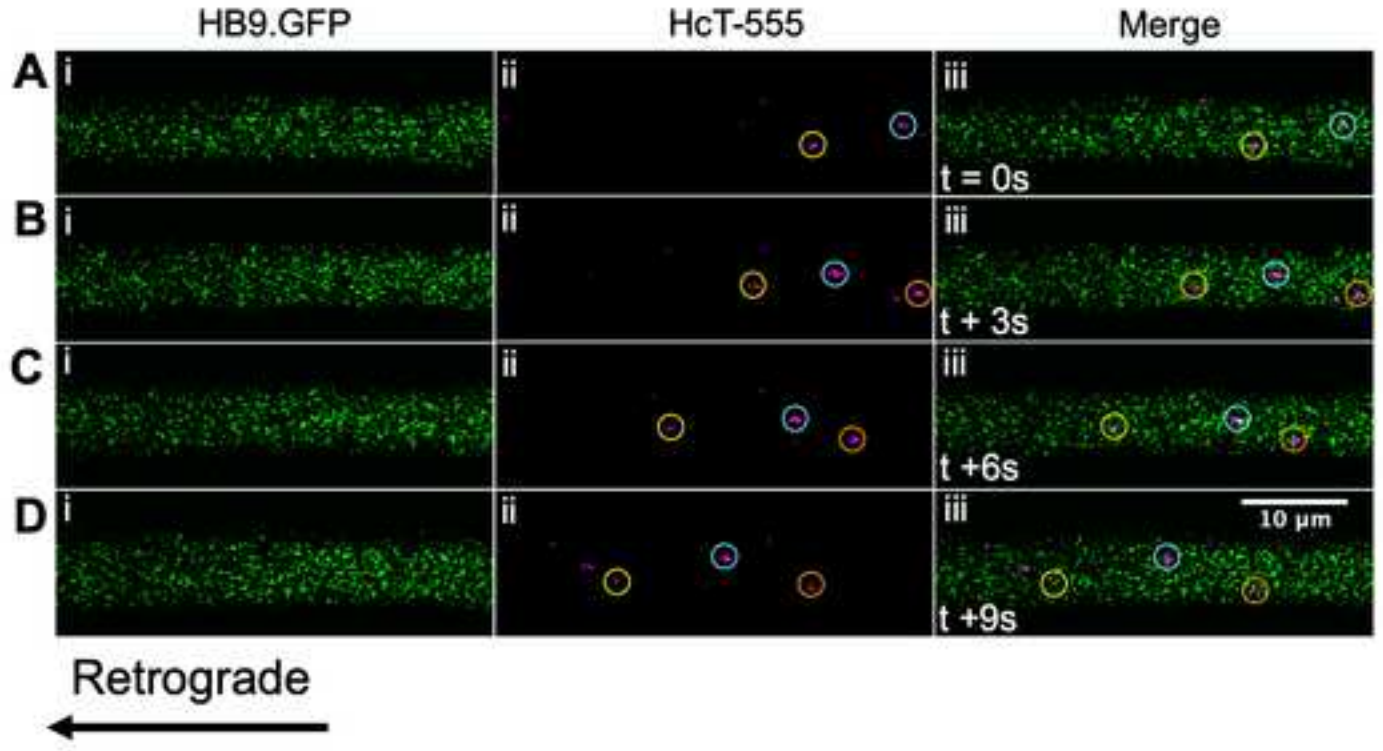

Figure 4

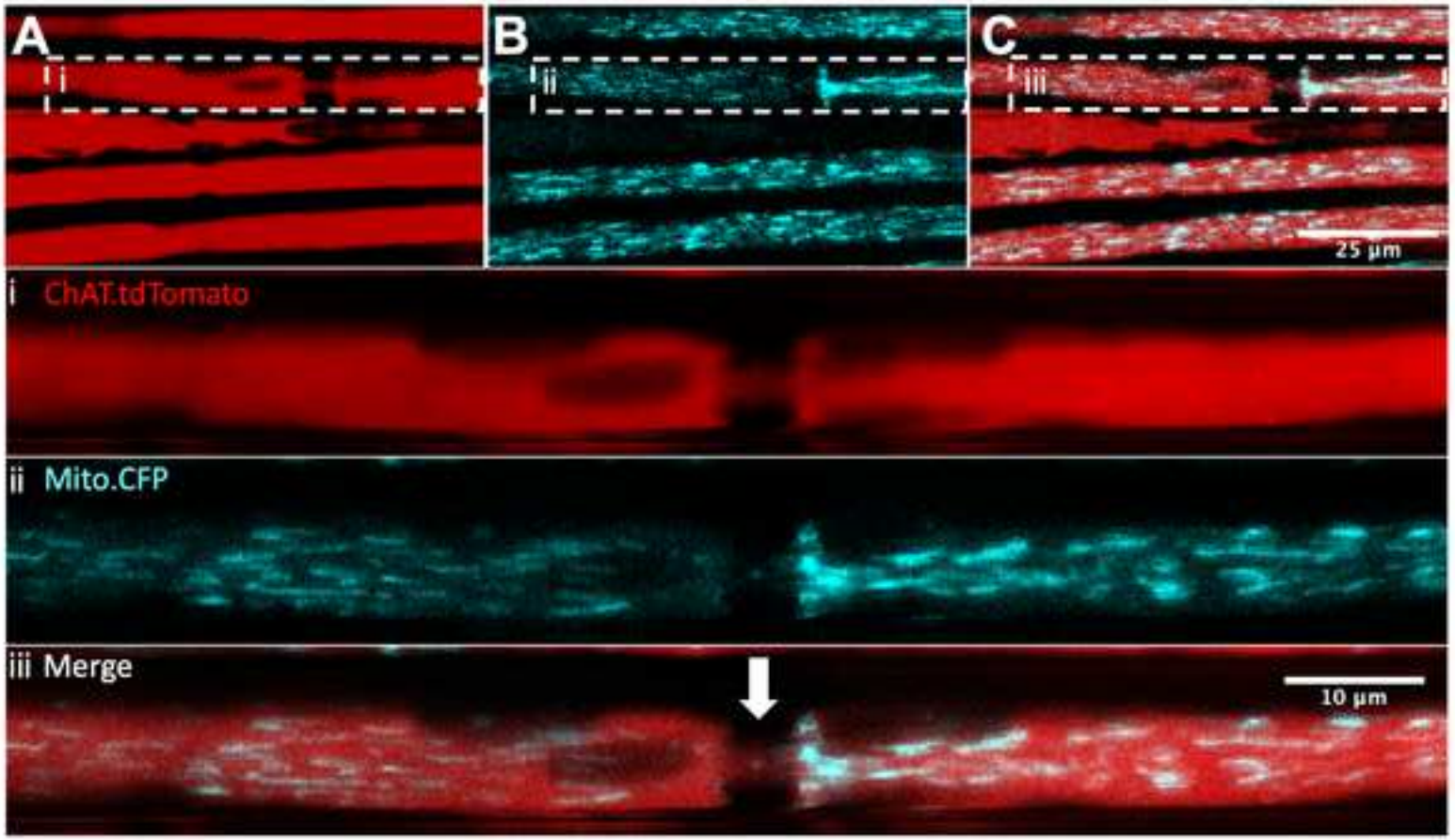

Figure 5

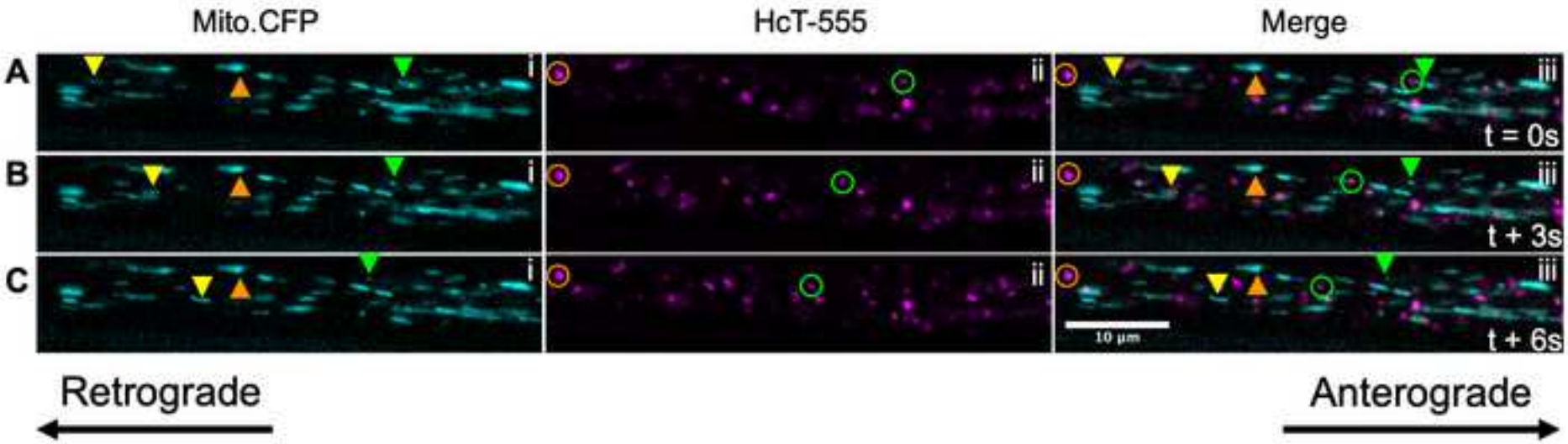

UCL INSTITUTE OF NEUROLOGY

THE NATIONAL HOSPITAL FOR NEUROLOGY AND NEUROSURGERY
QUEEN SQUARE
LONDON WC1N 3BG

Department of Neuromuscular Diseases
Head of Department: Professor Linda Greensmith

Andrew P. Tosolini, PhD
MNDA Junior Non-Clinical Research Fellow

29th November 2021

Vidhya Iyer, PhD
Review Editor,
JoVE

Dear Dr Iyer,

We are pleased to resubmit to JoVE our revised manuscript entitled "Expanding the toolkit for in vivo imaging of axonal transport (JoVE63471)" for your consideration.

The manuscript has been revised in response to all of the helpful comments and suggestions from yourself and both Reviewers.

Thank you for considering our manuscript.

Yours sincerely,

Andrew P. Tosolini, PhD
MNDA Junior Non-Clinical Research Fellow
Email: a.tosolini@ucl.ac.uk

James N. Sleigh, DPhil
MRC Career Development Fellow
Email: j.sleigh@ucl.ac.uk

Address for correspondence: Department of Neuromuscular Diseases, UCL Queen Square Institute of Neurology • National Hospital for Neurology and Neurosurgery (Box 28) • Queen Square • London WC1N 3BG.
☎ 07919 178756 • Fax: 020 7813 3107 • Email: a.tosolini@ucl.ac.uk •

Director: Professor Michael G Hanna BSc(Hons) MBChB(Hons) MD FRCP(UK)

Editorial comments:

Changes to be made by the Author(s):

1. Please take this opportunity to thoroughly proofread the manuscript to ensure that there are no spelling or grammar issues. Please define all abbreviations at first use.

We have given the manuscript several more proofreads.

2. Please provide an email address for each author.

We now include email addresses for all authors

3. Please revise the text, especially in the protocol, to avoid the use of any personal pronouns (e.g., "we", "you", "our" etc.).

We have removed all pronouns from the protocol section.

4. JoVE cannot publish manuscripts containing commercial language. This includes trademark symbols (TM), registered symbols (®), and company names before an instrument or reagent. Please remove all commercial language from your manuscript and use generic terms instead. All commercial products should be sufficiently referenced in the Table of Materials and Reagents.For example: MMRRC Stock Number: 000296-UCD; Jackson Laboratory Stock Number: 005029; Jackson Laboratory Stock Number: 007967; Jackson Laboratory Stock Number: 006410; Zeiss Zen;

We have done as asked.

5. Please ensure that all text in the protocol section is written in the imperative tense as if telling someone how to do the technique (e.g., “Do this,” “Ensure that,” etc.). The actions should be described in the imperative tense in complete sentences wherever possible. Avoid usage of phrases such as “could be,” “should be,” and “would be” throughout the Protocol. Any text that cannot be written in the imperative tense may be added as a “Note.” However, notes should be concise and used sparingly. Please include all safety procedures and use of hoods, etc.

We have amended text to use only the imperitive tense in the protocol section.

6. Please note that your protocol will be used to generate the script for the video and must contain everything that you would like shown in the video. Please ensure you answer the “how” question, i.e., how is the step performed? Alternatively, add references to published material specifying how to perform the protocol action. Please ensure the inclusion of specific details (e.g., button clicks for software actions, numerical values for settings, etc) to your protocol steps. There should be enough detail in each step to supplement the actions seen in the video so that viewers can easily replicate the protocol.

We have done as asked.

7. Please format the manuscript as: paragraph Indentation: 0 for both left and right and special: none, Line spacings: single. Please include a single line space between each step, substep, and note in the protocol section. Please use Calibri 12 points and one-inch margins on all the side. Please include a ONE LINE SPACE between each protocol step and then HIGHLIGHT up to 3 pages of protocol text for inclusion in the protocol section of the video.

We have done as asked

8. Please move the legends section to appear after the representative results section.

We have done as asked

9. Please add all items (plasticware, glassware, buffers, solvents, equipment, software etc) in the Table of Materials so that it serves as a handy reference for users to get everything ready for the protocol. Please sort the Materials Table alphabetically by the name of the material.

We have done as asked

Reviewer #1:

Manuscript Summary:

In the present manuscript Tosolini and colleagues describe in detail a method for in vivo imaging of axonal transport, and especially of signaling endosomes and mitochondria. Interestingly, by utilizing a mouse genetic approach, the authors could visualize organelles and cargoes while differentiating between motor and sensory axons.

Since axonal transport in motor and sensory neurons is known to be differentially impaired in neurodegenerative and neurodevelopmental disorders, in my opinion this method is of interest for the field.

Major Concerns:

There are no major concerns.

Minor Concerns:

-Line 267, also recommended numerical aperture for the objectives should be stated.

We have now included these details.

Lines 263-265 – “Either the 40x, 1.3 NA DIC Plan-Apochromat or 63x, 1.4 NA DIC Plan-Apochromat oil-immersion objectives can be used to image *in vivo* transport in the sciatic nerve.”

-The images shown in figure 1 are supposedly taken at the same magnification, however, the length and the thickness of the axons seem different. Is there a reason for it?

This distinction arises due to the age/size of the animals use to generate the two images. Therefore, the following text has been added to the legend of Figure 1:

Line 372: “Distinctions in axon calibre result from differences in mouse age and size.”

-In figure 3, motor axons visualized utilizing the Hb9GFP reporter look fragmented and not continuous (especially when compared to the ChatGFP and the ChatTdt shown in the previous images). Is this reporter dependent?

This is an interesting observation and one we cannot currently explain. However, we have included the following text (lines 616-617) to highlight this:

Lines 338-339: “Note that, unlike ChAT-driven expression, GFP has a more punctate/granular pattern in HB9.GFP axons – the reason for this is unclear.”

Reviewer #2:

Manuscript Summary:

Tosolini et al described a method to image axonal transport in vivo using transgenic animals and organelle markers. The focus on axonal transport, a critical cellular process for neuronal health and disease, is interesting to the field. While many assays exist to measure axonal transport in vitro, it is still challenging to quantify specific cargos in live animals. Therefore, this manuscript addresses an important knowledge gap. By using ChAT.tdTomato mice crossed with mito-CFP mice and fluorescent HcT, they were able to perform multiplexed imaging to track mito and signaling endosomes in motor vs. sensory neurons. Altogether, they have provided a useful platform to distinguish motor from sensor neurons by cell types specific reporter proteins; to measure transport of signaling endosomes in mice under anesthesia; to measure mito transport in motor neurons in vivo; and to co-measure signaling endosomes and mito in the same axon. While the assays are well described and details, like limitations, application, and critical steps, are well discussed, quantitative analysis should be better described and results be discussed in more detail. Finally, anesthesia has effects on axonal transport, though anesthesia is inevitable for this set of experiments, this needs to be discussed. However, these are minor details and don't dampen the enthusiasm for the manuscript, which is both interesting and useful to the neuroscience field.

Major Concerns:

1. It is important to describe the camera settings, particularly the imaging speed, as different cargoes can move at various speeds, undersampling using low fps has caused artefacts and misinterpretations of the transport velocity in the axonal transport field. It will be interesting to compare the speed of cargoes measured in vivo with that in vitro.

We thank the reviewer for this excellent comment and for highlighting this omission from our protocol. We agree that the frame rate should vary dependent upon the cargo being imaged. For example, signalling endosomes undergo fast axonal retrograde transport and have mean velocities of ~2.6 µm/s *in vivo* (Sleigh et al., 2020 *Cell Rep.* 30, 3655–3662.e2), and, as such, imaging should be performed at fast acquisition rates (e.g., 0.33-2 frame/s). Importantly, the mean velocities of signalling endosomes *in vivo* from wild-type mice were equivalent whether the frame acquisition rate was 0.5 s (Fellows et al., 2020 *EMBO Reports* 21 (3), e49129) or 3 s (Sleigh et al., 2020 *Cell Rep.* 30 (11), 3655–3662.e2). On the other hand, *in vivo* mitochondrial transport is much slower with mean velocities of ~0.5 µm/s (Bilsland et al., 2010 *PNAS* **107** (47), 20523–20528), and, as such, will require slower acquisition rates (e.g., 0.12-0.33 frame/s). What is critical is that the frame acquisition rate remains consistent across the entire axonal transport experiment/project as fluctuations in frame rates will likely cause biases within the data. We have therefore included the following relevant details in the manuscript.

Lines 297-299: “It is essential that the frame acquisition rate remains consistent across comparable datasets, because imaging at different frequencies may cause inconsistencies.”

We have previously compared in vitro vs. in vivo axonal transport of endosomes (Gibbs et al. 2016 *J. Neurosci Meth* **257**, 26–33) and have discussed in detail why

distinctions may arise (Sleigh et al. 2017 *F1000 Res* **6**, 200). We refer to this at the end of the fourth Introduction paragraph (i.e., lines 83-94).

2. Protein expression levels and fluorescent marker concentrations should be noted.
We thank the reviewer for allowing us to clarify this point. The only signalling endosome marker we used was fluorescent H_CT. We have successfully observed typical motile signalling endosomes after injecting 2.5-10 µg/µl of H_CT intramuscularly. As described in *1.1* #2 – the volume injected per muscle needs to be considered as smaller muscles cannot handle the larger volumes that are necessary to access the majority of pre-synaptic terminals at NMJs. We have also provided the fluorescent marker concentrations of the failed probes in the "Limitations of the technique" paragraph in the discussion – (lines 480-485; lines 491-497).

Minor Concerns:
1. Why certain organelle markers (e.g. lysosome) are not successful should be discussed. Is that just a concentration problem as briefly mentioned? If so, do other concentrations work? If not, are there other ways to measure those cargoes, using transgenic animals or other optogenetic tools for example?

We thank the reviewer for addressing this issue and agree that it requires a longer discussion. We used Lysotracker following Sasaki et al., (2014 PLoS Genet 26;10:e1004409), which labelled whole zebrafish embryos, BODIPY-FL-pepstatin A following Baltazar et al., (2012, 7:e49635), which labelled ARPE-19 cells and Magic Red following the manufacturer's instructions, with TMRE concentrations as reference for a probe that successfully labels organelles in the sciatic nerve *in vivo*. The probes labelled the nerve, but mainly in Schwann cells, therefore the lack of signal in vesicular compartments may also be due to the inability of the probes to reach the neurons. We cannot rule out that different concentrations might result in a better delivery of the probes. We have added this possibility to the "limitations of the technique" section.

Currently, most studies tracking lysosomes in neurons use *in vitro* approaches (Ferguson 2018, *Curr Opin Neurobiol* 51:45-51), however it would be possible to study their intravital axonal transport with mouse models carrying fluorescently tagged lysosomal markers, such as LAMP-1. We have also added this alternative and its caveat to the "other potential applications" section.

Lines 497-500: "The probes accumulated around axons, likely being retained in Schwann cells, hence the unsuccessful labelling of lysosomes may arise from deficient probe delivery into neurons, although the existence of more suitable concentrations cannot be ruled out."

Lines 535-537: "Furthermore, the lysosomal labelling difficulties can be surpassed using mice expressing LAMP1-GFP, with the caveat that LAMP1 is also present in endocytic organelles different from lysosomes [74]."

2. The effects of anesthesia should be acknowledged and discussed
This is another excellent point that we have now addressed. The effects of anesthesia on axonal transport of signalling endosomes and mitochondria are largely unknown. The only study to investigate this revealed that the axonal transport dynamics of dense core vesicles from the superficial cortical layers are similar in anesthesited and awake

mice (Knabbe et al., 2018 *J Phys* 596, 3759–3773). However, whether all methods of anesthesia elicit the same lack of influence on transport dynamics is unknown, especially as certain physiological readouts (e.g., cochlea function (Cederholm et al., 2012, *Hearing Res.* 292, 71–79) and cortical electrophysiology (Michaelson and Kozai, 2018, *J Neurophys* 120, 2232–2245) differ depending upon the method used (e.g., isoflurane vs ketamine/xylazine/acepromazine). We have included these points in the “Limitations of the technique’ section in the discussion.

Lines 506-515: “Methods of anesthesia can alter distinct physiological readouts (e.g., cochlea function [63] and cortical electrophysiology [64]); however, whether anesthesia influences axonal transport in the sciatic nerve is currently unknown. Given the reduced neuromuscular activity under isoflurane-induced anesthesia, it is possible that transport kinetics differ compared to the wakeful state. However, the only *in vivo* study that has directly investigated this revealed that transport of dense core vesicles in thalamocortical projections does not differ between anesthetized and awake mice [65]. Furthermore, since distinctions in transport between wild-type and disease model mice are detectable under anaesthesia [35,43], it is clear that isoflurane exposure does not prevent identification of perturbances in signalling endosome or mitochondrial trafficking.”